INFLUENCE OF SURFACE-CONDUCTIVITY DISTRIBUTION ON CHARGE ACCUMULATION OF GIS INSULATOR UNDER DC FIELD

H. Iwabuchi[1], T. Donen[1], S. Matsuoka[1], A. Kumada[1], K. Hidaka[1], M. Takei[2], and Y. Hoshina[2]
[1] Department of Electrical Engineering, The University of Tokyo,
7-3-1, Hongo, Bunkyo-ku, Tokyo 113-8656 JAPAN
[2] Power Systems Company, Toshiba Corporation,
2-1, Ukishima-cho, Kawasaki, Kanagawa 210-0862 JAPAN
*Email: <iwabuchi@hvg.t.u-tokyo.ac.jp>

Abstract: When a dc voltage is applied to an insulating spacer, the electric field distribution around it is determined by the resistivity of the material. Consequently, charges are accumulated on the surface of the insulator, and the breakdown voltage of it can become low. In this paper, the charge density distribution of the insulator is measured. An electrostatic probe is set close to the measured object and scans along its surface keeping a small gap. From the measured data, the accumulated charge is inversely calculated by utilizing the relationship between the charge and the potential profile which is obtained by numerical electric field computation. The authors assume that the surface leakage current is the main factor of the charge accumulation. Therefore, the influence of the surface conductivity on the charge accumulation is examined from both sides of experiment and numerical computation. It is confirmed that non-uniform surface conductivity is responsible for the charge accumulation.

1 INTRODUCTION

In a gas-insulated switchgear (GIS), a dc voltage occasionally remains on the bus bar when the switchgear works. If a dc voltage is applied for an insulating material inside GIS for a long time, the electric field distribution around it changes from the initial capacitive distribution to a resistive distribution, which is determined by the resistivity of the material. Consequently, charges are accumulated on the spacer surface. For designing a highly reliable electric power apparatus, it is indispensable to get information on this accumulated charge distribution.

An electrostatic probe is generally utilized for measuring surface charge distribution on an insulating material such as downsized simple models of post type spacers [1,2]. Due to the instability of the inverse calculation from the probe outputs to the charge distribution, the numbers of measured points was a few hundred at the best, and the spatial resolution was worse than 10 mm [2]. Recently, signal processing techniques have been adopted to improve the stability of the inverse calculation, and the spatial resolution has been improved to mm order [3].

In this paper, the charge distribution on an epoxy-resin disc spacer in SF6 is measured and the result shows that the surface leakage current is the main factor of the charge accumulation. Therefore, correlation between the surface conductivity and the charge distribution is investigated.

2 CHARGE DISTRIBUTION MEASUREMENT

2.1 Matrix equation of transfer characteristics

An electrostatic probe is set close to the spacer and scans along its surface keeping a small gap. The potential of a sensing electrode is determined by all the accumulated charge on the measured object. The probe output, therefore, corresponds to a linear superimposition of the effect of the charge.

As shown in Figure 1, the surface of the measured object is divided into N elements. When each elements is charged with $q_i = s_i\sigma_i$, where σ_i is the surface charge density and s_i is the element area, the probe response w_j obtained above the center of gravity of an element j is expressed as follows

$$\begin{pmatrix} w_1 \\ \vdots \\ w_N \end{pmatrix} = \begin{pmatrix} h_{11} & \dots & h_{1N} \\ \vdots & \ddots & \vdots \\ h_{N1} & \dots & h_{NN} \end{pmatrix} \begin{pmatrix} q_1 \\ \vdots \\ q_N \end{pmatrix} \tag{1}$$

The matrix component h_{ij} of Eq. 1 is the probe response at the point i caused by a unit charge at the element j. The N^2 components of this matrix are calculated by the numerical electric field computation, using the triangular surface charge method with a linear representation of the element-shape and a constant representation of the charge density on an element. In this study, the number of field computation for N^2 components (N=6846) is reduced to 172 by considering the geometric symmetry of the measured object and by the reciprocity principle for the relation between charge *Q* and potential *V* [4]

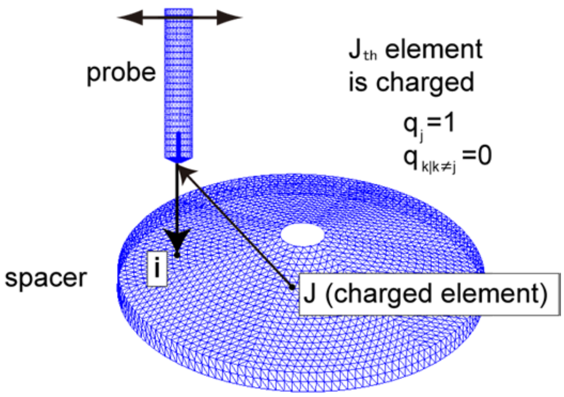

Figure 1. Surface of the measured object divided into *N* elements.

2.2 Signal processing technique

Noise is usually identified in the measured data. To reduce the influence of the noise in the inverse calculation process as expressed by Eq. 1, the signal processing technique using a Tikhonov's regularization [5], which is based on the minimum mean-square error criterion, is practically adopted. Assuming that there is no correlation between the signal and the noise, the estimated solution of *q* is given by

$$\mathbf{q} = \left([H]^T [H] + \frac{\sigma_n^2}{\sigma_s^2} [I] \right)^{-1} [H]^T \mathbf{w} \qquad (2)$$

where [*H*] is a coefficient matrix of Eq. 1, [I] is a unit matrix, $\mathbf{q} = (q_1, ..., q_N)^T$, $\mathbf{w} = (w_1, ..., w_N)^T$, and σ_n and σ_s are standard deviations of the noise and the signal respectively. Under most circumstances, however, the precise ratio of the variances given by $\gamma = \sigma_n / \sigma_s$ is unknown. In this study, γ is set at 0.3% of the largest eigen value of the matrix $[H]^T[H]$ on an empirical basis. The spatial resolution of the measuring system, including the inverse calculation, is 5.4 mm.

2.3 Experimental setup

Figure 2 shows the side view of a downsized GIS bus bar which consists of a central rod electrode, a grounded cylindrical electrode, and an epoxy-resin (relative permittivity ε_r= 5.93) spacer. The spacer base diameter is 90 mm, and its height is 15 mm, which has a sloping top surface and a flat bottom surface. The spacer is set between cylindrical electrodes, and a dc voltage is applied to a central electrode. After the removal of a dc voltage, the spacer is removed from the bus bar model, and set at the surface charge measuring system as shown in Figure 3. The electrostatic probe consists of a sensing electrode of 1 mm diameter and a grounded guard electrode which has a hole of 2 mm diameter for the sensing electrode. The electrostatic probe moves along the surface of the spacer, maintaining a gas gap of 1 mm. The sloping surface of the spacer is divided into 3444 triangular elements, and the flat surface into 3402 elements. The potential of the sensing electrode at the center of each element is measured by a voltmeter with high input impedance. To improve dust control, all experimental setups are put in a sealed container filled with SF_6 gas at atmospheric pressure. Before the voltage application, the dry process was done in an environmental test chamber at a temperature of 80 ℃ and at a humidity of 30% for 24 hours.

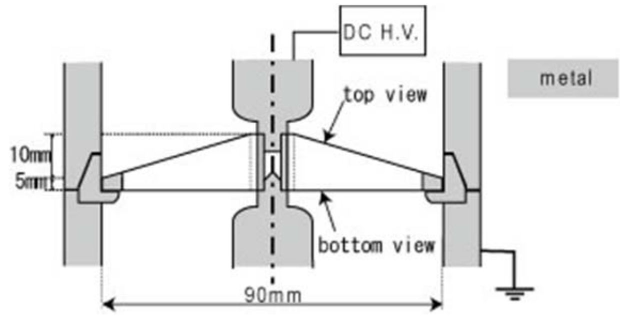

Figure 2. Side view of a disc spacer and the electrodes.

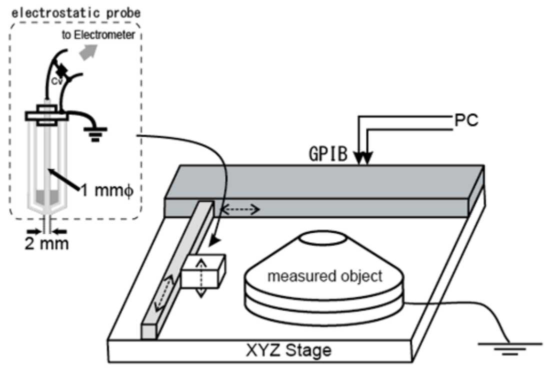

Figure 3. Schematic diagram of the charege measuring system.

2.4 Experimental result

A dc voltage was applied to a central electrode for 280 hours and the accumulated charge density was measured. After the voltage application, the central electrode was grounded and the decay of the charge density was measured every 24 hours. The voltage application and the scanning process were conducted on four disc spacers simultaneously, which were numbered as spacer1 to spacer4.

Figures 4 and 5 show the charge distribution obtained after 280 hours voltage application of 30 kV. Although there were individual differences, more accumulated charges were observed on the flat surface than on the sloping surface of all spacers.

Figure 6 shows temporal change of the charge density on an element of the flat surface, where the maximum charge density was measured after 280 hours voltage application. The time constant of charge accumulation was over 100 hours.

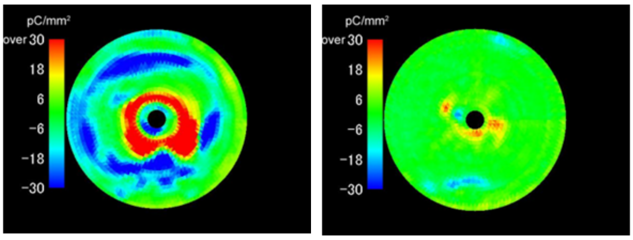

(a) Spacer1 (b) Spacer2

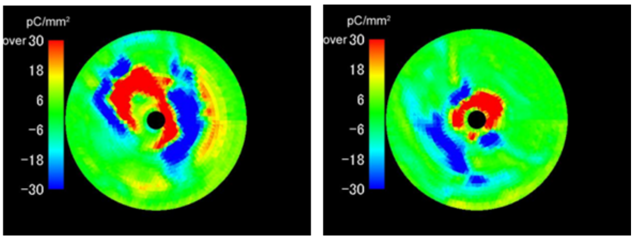

(c) Spacer3 (d) Spacer4

Figure 4. Charge distribution after 280 hours voltage application on the flat surface of the spacer.

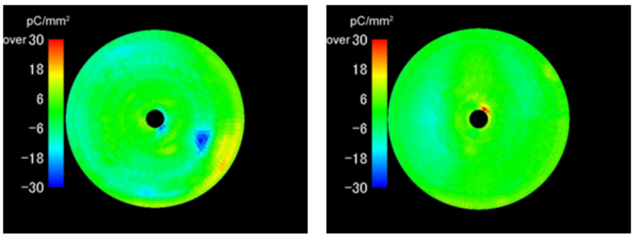

(a) Spacer1 (b) Spacer2

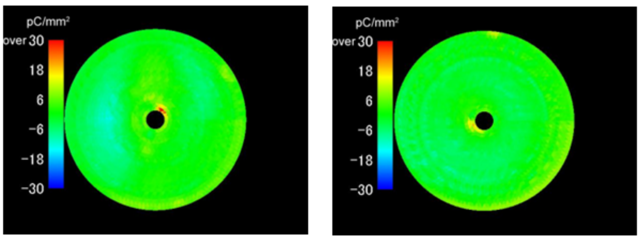

(c) Spacer3 (d) Spacer4

Figure 5. Charge distribution after 280 hours voltage application on the sloping surface of the spacer.

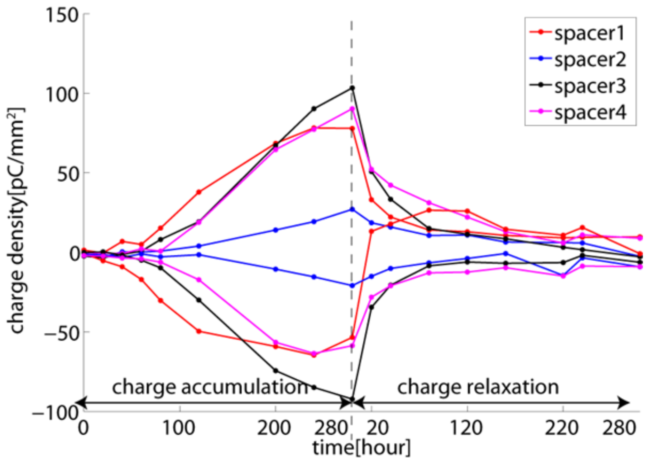

Figure 6. Temporal change of charge density.

As shown in Figure 4(a), some concentric charge-patterns were also observed. These axisymmetric charge-patterns may be caused by the following factors; the electric conduction along the surface of the insulator, the electric conduction through the volume of the insulator, and the adhesion of charge generated by electric field emission.

The maximum electric field intensity on the surface of centre electrode stressed by 30kV was calculated to be 3.1kV/mm, which is substantially smaller than the required value for electric field emission. Moreover, if the electric field emission takes place, the time constant of charge accumulation must be shorter. Therefore, the electric field emission is not the main factor of charge accumulation in this experiment.

As the volume conductivity of epoxy is small and its relaxation time is much longer, it is natural to say that the surface leakage current is the main factor of the charge accumulation.

3 CHARGE DISTRIBUTION MEASUREMENT OF ROUGHED SPACER

Charge accumulation on the spacer is mainly affected by the conduction along the surface of the spacer, as pointed out in subsection **2.4**. The charge accumulation, whose surface was concentrically roughed by sand blast process as shown in Figure 7, was measured. The surface conductivity changes with the sand blast process because filler of the spacer appears on the surface of the spacer.

After the 240 hours voltage application, the charge distribution of the spacer with roughed surface is shown in Figure 8. On the flat surface of the spacer, charges were accumulated along the boundary of the roughed region, as marked with broken line in Figure 8. More accumulated charges were observed on the flat surface of the spacer than on the sloping surface of the spacer.

The temporal change of the charge density on an element of the flat surface, where the maximum charge density was measured after 240 hours voltage application, is shown in Figure 9. Maximum charge density was 100pC/mm^2, which is similar amount as observed on spacer 1 to 4 shown in Figure 6. It is possible to say that the charge accumulation in this study is mainly affected by the non-uniformity in surface conductivity.

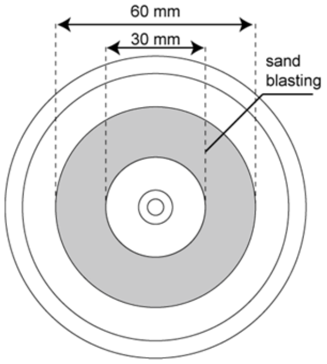

Figure 7. Sand blasted region on the spacer.

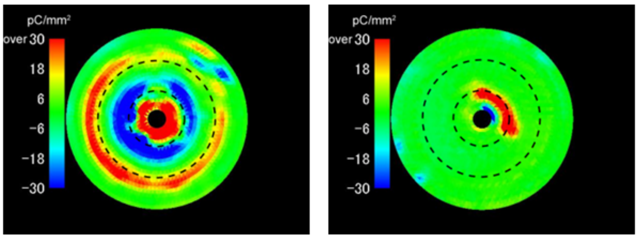

(a) Flat surface **(b) Sloping surface**

Figure 8. Charge distribution after 240 hours voltage application for the spacer with non-uniform surface conductivity.

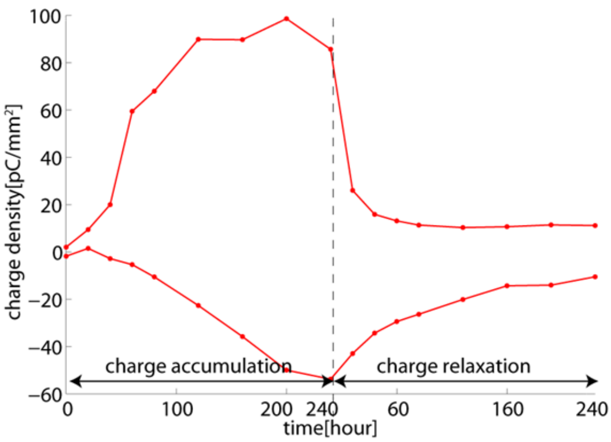

Figure 9. Temporal change of charge density on the spacer with non-uniform surface conductivity.

4 NUMERICAL SIMULATION OF CHARGE ACCUMULATION

4.1 Simulation model

The accumulation of charge was simulated based on electric field computation with charge simulation method (CSM) taking surface and volume conductivities into account. Calculation model is shown in Figure 10(a), which simulated the experimental setup shown in Figure 2, where σ_{Epoxy} is the volume conductivity of epoxy resin, σ_{SF6} is that of SF6, and σ_S is surface conductivity between epoxy resin and SF6. Relative permittivity of epoxy resin is 5.93 and that of SF6 is 1. Surface conductivity distribution, as shown in Figure 10(b), is partially high in the region of 15mm < r <30mm, which corresponds to the sand blasted region shown in Figure 2. A step voltage of 30kV is applied to the central electrode.

The applied voltage waveform is expanded into a Fourier series, and the electric field distribution for each frequency component is numerically calculated by the charge simulation method with complex permittivity. The transient change in the electric field distribution is obtained by combining back these frequency components.

The accumulated surface charge density on the spacer surface is calculated by applying Gauss's law as follows:

$$\sigma = \varepsilon_g E_{gn} - \varepsilon_{Epoxy} E_{Epoxyn} \quad (3)$$

where ε_g and ε_{Epoxy} are the permittivities of the gas and the spacer, E_{gn} is the normal component of the electric field in the gas, and E_{Epoxyn} is that in the spacer.

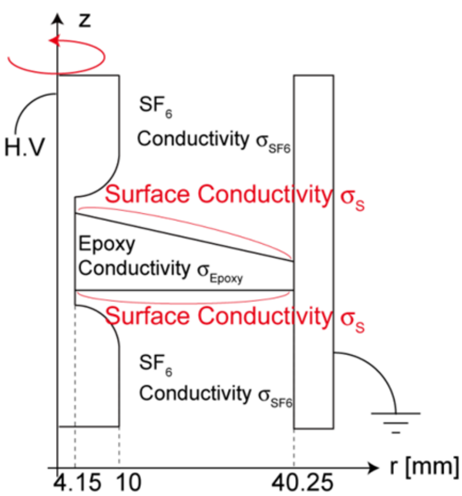

(a) Calculation model.

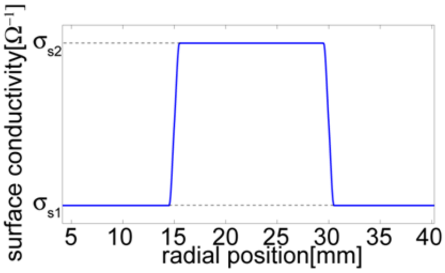

(b) Surface conductivity distribution on the spacer

Figure 10. Calculation condition

4.2 Accumulated charge under dc field

When prolonged dc voltage is applied to the material, the electric field distribution changes from an initial capacitive distribution to a resistive distribution, and consequently, charges are accumulated on the material surface. Figure 11 shows the accumulated charge distribution on spacer surfaces where the electric field forms resistive distribution under such a condition that the ratio of $\sigma_{SF6}/\sigma_{Epoxy}$ is set at 10^{-1} ,10^{-2} ,10^{-3} ,10^{-4} and σ_S=0. The maximum charge density is 10pC/mm^2, which is considerably smaller than the experimental one. This result verifies the assumption that the surface leakage current is the main factor of the charge accumulation.

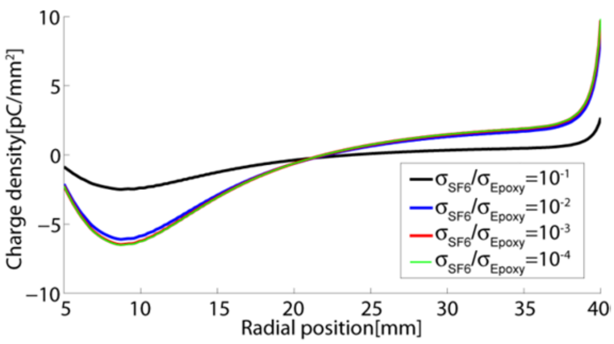

(a) On the flat surface of the spacer.

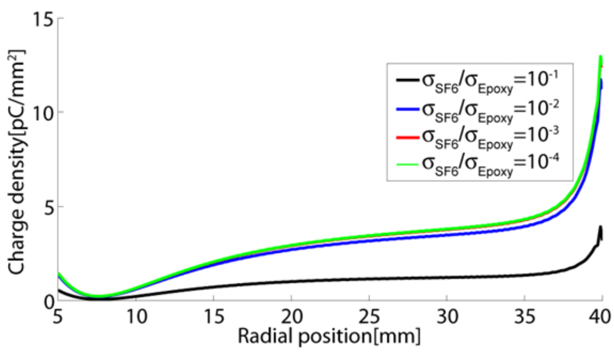

(b) On the sloping surface of the spacer.

Figure 11. Charge density distribution considering only volume conductivity

4.3 Simulation considering only surface conductivity

Figure 12 shows the accumulated charge distribution on spacer surfaces where the electric field forms resistive distribution under such a condition that the volume conductivities of gas and spacer are 0 and the surface conductivity σ_S distributes a profile shown in Fig. 10(b). Charges are accumulated along the boundary at *r*=15 and 30mm, where the surface conductivity changes drastically.

The amount and the polarity of the charge is associated with the ratio between σ_{s1} and σ_{s2}. When σ_{s1}/σ_{s2} is high, more positive charge is accumulated at *r*=15mm, and more negative charge, at *r*=30mm. On the other hand, when σ_{s1}/σ_{s2} is low, more negative charge appears at *r*=15mm, and more positive charge, at *r*=30mm. The accumulated charge density on the boundary of the roughed region is approximately 100pC/mm^2 as described in section 3, therefore, it is possible to estimate the ratio σ_{s1}/σ_{s2} of the spacer used in this study to be 5.

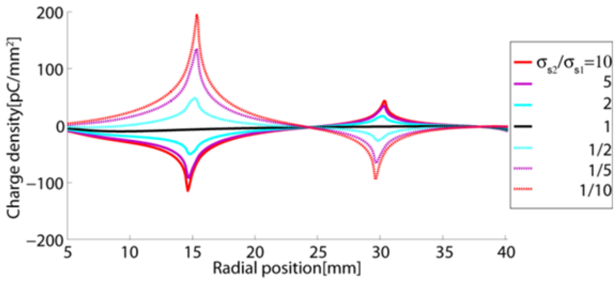

(a) On the flat surface of the spacer.

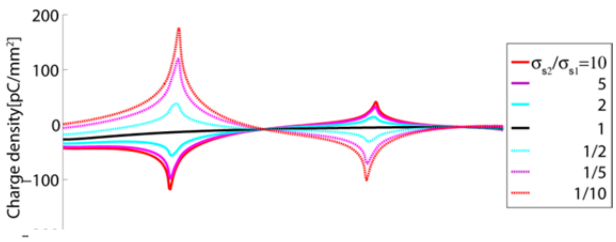

(b) On the sloping surface of the spacer.

Figure 12. Charge density distribution considering only surface conductivity

4.4 Transient change in accumulated charge

Figures 13 and 14 show the transient change in the electric field distribution and the accumulated charge distribution, respectively. Calculation condition was as follows; Surface conductivity σ_{S1} was set at $10^{-18}\,\Omega^{-1}$ and σ_{S2} was set at $5\times10^{-18}\,\Omega^{-1}$.

The volume conductivity σ_{Epoxy} was set at 1×10^{-16} $\Omega^{-1}m^{-1}$ [6] and the ratio $\sigma_{SF6}/\sigma_{Epoxy}$ was 10^{-2}.

After the 20 hours voltage application, the electric field intensity is temporarily higher than initial distribution along the boundary of the roughed region.

The negatively charged region appears at *r*=15mm and the positively charged region appears at *r*=30mm, and firstly the peak values increase rapidly. When 10 hours passes, the maximum charge density exceeds over 50pC/mm^2 on the boundary of the roughed region and the electric field intensity on it takes temporally the highest value. With time passes, the charged region expands and the electric field on the boundary is relaxed. Time constant of charge accumulation was over 100 hours, which coincides well with the experimental results shown in Figure 9. Therefore, the surface conductivity of the disc spacer was estimated to $10^{-18}\,\Omega^{-1}$ in dried environment.

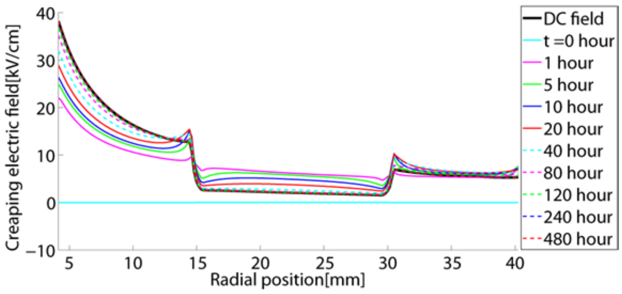

Figure 13. Temporal change of electric field intensity on the flat surface of the spacer.

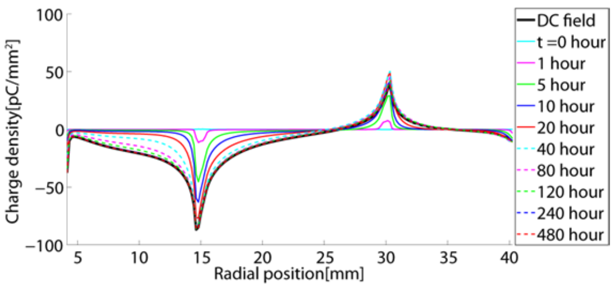

Figure 14. Temporal change of charge density on the flat surface of the spacer.

5 CONCLUSION

The charge distribution on the spacer surface was measured after 280 hours voltage application of +30 kV. The result indicates that the surface leakage current is the main factor of the charge accumulation. As the surface leakage current is considered to be affected by the surface conductivity, the charge accumulation on spacer, whose surface was partially roughed with a sandblast process, was also measured. In this case, the charge density was high on the boundary of the roughed area.

In addition, charge accumulation was simulated based on electric field computation with charge simulation method taking surface and volume conductivity into account. In the case that only the volume conductivity was taken into account, simulated charge density was considerably smaller than the experimental one. This result verifies the assumption that the surface leakage current is the main factor of the charge accumulation. Temporal change of the accumulated charge distribution was also simulated in the case of the roughed spacer. The simulated result shows that the charge density is relatively high on the boundary of the roughed area. It coincides well with the experimental results.

6 REFERENCES

[1] H. Fujinami, T. Takuma, M. Yashima, and T. Kawamoto, "Mechanism and Effect of dc Charge Accumulation on SF6 Gas Insulated Spacers", IEEE Trans. Power Del., Vol. 4, 1989, pp. 1765-1772.

[2] S. Okabe, T. Okada, S. Yuasa, T. Utsumi, F. Endo, and K.Saitoh, "Effect of dc Prestress on Dielectric Characteristics of an Insulator in SF6 gas", Proc. of the 12th Intern. Sympos. Vol. 2, 2001. pp. 351-354.

[3] A. Kumada, and S. Okabe, "Charge Distribution Measurement on a Truncated Cone Spacer under dc Voltage", IEEE Trans. Dielect. Electr. Insul., Vol. 11,2004, pp.929-938.

[4] A. Pedersen, "On the Electrostatics of Probe Measurements of Surface Charge Densities", in: L. G. Christophorou and D. W. Bouldin .Eds.., Gaseous Dielectrics V, 1987, pp. 235-241.

[5] W. K. Pratt, "Digital Image Processing", John Wiley & Sons, Inc., 1987, U.S.A, pp. 378-388.

[6] S. Okabe, "Phenomena and Mechanism of Electric Charges on Spacers in Gas Insulated Switchgears", IEEE Transactions on Dielectrics and Electrical Insulation, Vol.14, No.1, pp.46-52, 2007